(2)

UNCLASSIFIED
SECURITY

AD-A201 444 ENTATION PAGE

Form Approved
OMB No. 0704-0188

1a. REPC
UNC

1b. RESTRICTIVE MARKINGS

DTIC FILE COPY

2a. SECURITY CLASSIFICATION AUTHORITY

ELECTE
NOV 15 1988
D

3. DISTRIBUTION / AVAILABILITY OF REPORT

Approved for public release;
Distribution is unlimited

2b. DECLASSIFICATION / DOWNGRADING SCHEDULE

4. PERFORMING ORGANIZATION REPORT NUMBER(S)

5. MONITORING ORGANIZATION REPORT NUMBER(S)

AFOSR-TR- 88-1319

6a. NAME OF PERFORMING ORGANIZATION	6b. OFFICE SYMBOL (If applicable)	7a. NAME OF MONITORING ORGANIZATION
Northwestern University		AFOSR/NC

6c. ADDRESS (City, State, and ZIP Code)	7b. ADDRESS (City, State, and ZIP Code)
Department of Chemistry 2145 Sheridan Road Evanston, IL 60208	Building 410 Bolling AFB, DC 20332-6448

8a. NAME OF FUNDING / SPONSORING ORGANIZATION	8b. OFFICE SYMBOL (If applicable)	9. PROCUREMENT INSTRUMENT IDENTIFICATION NUMBER
AFOSR	NC	AFOSR-83-0302

8c. ADDRESS (City, State, and ZIP Code)	10. SOURCE OF FUNDING NUMBERS			
	PROGRAM ELEMENT NO.	PROJECT NO.	TASK NO.	WORK UNIT ACCESSION NO.
Building 410 Bolling AFB, DC 20332-6448	61102F	2303	A2	

11. TITLE (Include Security Classification)

The Role of Surface Structural Defects in the Oxidation of Al(111) Surfaces

12. PERSONAL AUTHOR(S)

Stair, Peter Curran

13a. TYPE OF REPORT	13b. TIME COVERED	14. DATE OF REPORT (Year, Month, Day)	15. PAGE COUNT
Final	FROM 10/83 TO 7/88	November 1, 1988	26

16. SUPPLEMENTARY NOTATION

17. COSATI CODES			18. SUBJECT TERMS (Continue on reverse if necessary and identify by block number)
FIELD	GROUP	SUB-GROUP	
			Surface Defects, Surface Chemistry, ~~LEED~~ (ES) CRYSTALLOGRAPHY,

19. ABSTRACT (Continue on reverse if necessary and identify by block number)

The purpose of this research has been to identify atomic scale structural defects in metal single crystal surfaces and to determine the influence of these defects on surface oxidation. We have determined that atomic-height steps are the location for the nucleation of oxide on Al(111) surfaces and that surface diffusion to the steps is a critical step in the oxidation mechanism.

20. DISTRIBUTION / AVAILABILITY OF ABSTRACT	21. ABSTRACT SECURITY CLASSIFICATION
☒ UNCLASSIFIED/UNLIMITED ☐ SAME AS RPT. ☐ DTIC USERS	UNCLASSIFIED

22a. NAME OF RESPONSIBLE INDIVIDUAL	22b. TELEPHONE (Include Area Code)	22c. OFFICE SYMBOL
Lt Col James G. Scholz	(202) 767-4963	NC

DD Form 1473, JUN 86 — Previous editions are obsolete. — SECURITY CLASSIFICATION OF THIS PAGE

UNCLASSIFIED

88 12 22

THE ROLE OF SURFACE STRUCTURAL DEFECTS IN THE OXIDATION OF Al(111) SURFACES

AFOSR-TR- 88-1319

Peter C. Stair
Department of Chemistry
Northwestern University
Evanston, Illinois 60203

November 1, 1988

Final Report for Period September 1983 to July 1988

DISTRIBUTION UNLIMITED

Prepared for

AIR FORCE OFFICE OF SCIENTIFIC RESEARCH
Bolling Air Force Base, D.C. 20332-6448

A-1

RESEARCH OBJECTIVES

The research objectives associated with this project can be divided into three categories:

Develop low-energy electron diffraction (LEED) as a tool for quantitative analysis of extended and point surface structural defects.

Characterize the nature and concentration of defects produced by sputtering and annealing treatments of single crystal surfaces. A systematic examination of the defects produced by surface fabrication and cleaning procedures was needed to evaluate the effect of these treatments on surface properties.

Determine the influence of surface defects on surface chemistry. A central hypothesis of this research project was that surface defects strongly influence the rates of surface chemical reactions associated with oxidation and corrosion and the morphologies of resulting oxide layers. A comparison of the chemical behavior of relatively perfect, well annealed single crystal surfaces with surfaces having known defect structures was performed to prove this hypothesis.

RESULTS OF THE RESEARCH

Development of LEED Experimental Technique

An ultrahigh vacuum surface analysis apparatus was constructed with capabilities for quantitative LEED pattern measurements and quantitative surface oxidation rate measurements by Auger electron spectroscopy. A

schematic diagram of the apparatus is shown in Fig. 1. The sample is positioned in the center of the chamber. It is mounted on a high precision manipulator which permits accurate positioning of the sample along three translation axes as well as rotation about two axes, one in the sample plane and one normal to the sample plane. The LEED optics and a cylindrical mirror analyzer for Auger spectroscopy are mounted on two separate flanges that can be translated into the proper positions for sample analysis. The usual facilities for sputtering and gas introduction are provided. The entire vacuum system is pumped by a turbomolecular pump - titanium sublimation pump combination.

Four aspects of a LEED pattern can be measured quantitatively: 1) the positions of the diffracted electron beams; 2) the integrated intensity of each beam as a function of electron energy and/or angle of incidence on the surface; 3) the angular distribution of intensity within each beam, and 4) the angular distribution of intensity in the background between beams. The positions of the diffracted beams determine the reciprocal lattice which arises as a result of long range order on the single crystal surface. The integrated intensity of each diffracted beam as function of energy contains information on the atomic structure within each surface unit cell and must be analyzed by dynamical scattering theory [1]. The angular distribution of intensity within each beam can be analyzed in a kinematical approximation [2] as a function of energy and angle of incidence to determine the nature and density of extended surface structural defects such steps, mosaic boundaries, and strain [3-5]. The angular distribution of the background intensity (diffuse LEED) contains information on the structure of point defects in the crystal surface and can be analyzed via dynamical scattering theory [6]. The latter two measurements were the focus of this research project.

A unique feature of the experimental approach which facilitated quantitative LEED measurements of the entire diffraction pattern (background intensity distribution and beam angular profile) was a pulse counting, digital imaging electron optics depicted in Fig. 2. The phosphor screen in an otherwise ordinary display-type LEED optics has been replaced by a pulse counting, position sensitive electron detector. The detector consists of a 75-mm Chevron Channel Electron Multiplier Array for amplifying individual electrons into pulses and a resistive film anode for collecting the electron pulses. Associated electronics include charge sensitive, pulse shaping amplifiers and a pulse height ratio, position analyzer circuit. The electron detector is interfaced to a microcomputer through a pair of fast analogue to digital converters to accumulate a digital image of the electron diffraction pattern. The operation of this detector has been described previously [7].

Once a diffraction pattern has been collected, the image may be examined by a variety of computational procedures. For example, a contour plot of the entire diffraction pattern indicates the positions of all beams and the distribution of background intensity. Fig. 3 shows a contour plot of the LEED pattern from the clean, annealed Al(111) surface. The contour intervals and range have been chosen to emphasize structure in the background between beams. Note the overall hexagonal symmetry of the beam positions characteristic of the surface symmetry. Note also the hexagonal symmetry of the background intensity as well. The hole in the center of the pattern is where the incident electron beam passes through the detector via a shielded drift tube.

The presence of extended surface structural defects leads to angular broadening of the diffraction beams [4-5]. The experimental sensitivity to extended defects is determined by the instrument response function of the LEED optics [8,9] and varies with the type of defect. The sensitivity limits for

mosaic, step, and strain defects for the digital LEED instrument are 0.8%, 0.4%, and 0.4% respectively.

The background intensity which is the measurable quantity for diffuse LEED is very weak for a well ordered, single crystal surface. Furthermore, an implicit assumption in the analysis of diffuse LEED intensities is the absence of long range correlations to the surface structural unit which is responsible for the diffuse intensity. Experimentally, this condition is nearly impossible to achieve since the likely point defects, adatoms and vacancies, are located in identical sites on the surface which are automatically correlated by the surface periodicity. As discussed by Pendry and coworkers [6,10] these long range correlations primarily influence the structure factor which is energy independent. Therefore, if the data is presented in the form of a logarithmic derivative of the intensity with respect to energy, $L = d\ell nI/dE$, the structure factor and hence the influence of long range correlations cancels out. The most convenient form to compare calculation and experiment is the so-called Y-function defined by Pendry [6,10], $Y = L/(1 + L^2V^2)$, where V is the inner potential which can be taken as an adjustable parameter. An experimental determination of the Y-function involves 1) LEED intensity measurements at two closely spaced energies, 2) radial expansion of the higher energy data so that the k-space coordinates in the two measurements are aligned, 3) smoothing of the data to remove artificial structure caused by the retarding grids and imperfections in the electron detector, and 4) calculation of the Y-function. The smoothing performed to remove grid structure is the most critical step in the data reduction procedure because any sharp features which remain in the data are amplified when calculating the Y-function. The grid structure is evident in Fig. 4 which shows two slices from an image of the Al(111) LEED pattern taken

before and after adsorption of oxygen. Clearly, what appears to be noise is not statistical but is reproduced in both sets of data.

The grid structure can be removed with minimal loss of information using an optimized two-dimensional Fourier smoothing procedure described by Stark and Dimitriadis [11]. The usual procedure for smoothing two-dimensional intensity data is to convolve the measured intensity function, $I(x,y)$, with a window function $W(x,y)$ to generate a smoothed intensity function, $I_W(x,y)$:

$$I_W(x,y) = \int_{-\infty}^{\infty} \int_{-\infty}^{\infty} I(x-x',y-y')\, W(x',y')\, dx'\, dy'$$

Fourier techniques are used to implement the convolution. Stark and Dimitriadis showed that an optimized window function may be selected to minimize distortion of the data for a given amount of smoothing. This two-dimensional function with assumed radial symmetry has the following form:

$$W_o(\rho) = 4\pi c^2 \zeta_1^2 \{J_o^2(2\pi\rho c)/[\zeta_1^2 - (2\pi\rho c)^2]^2\}$$

where ρ is the radial coordinate of the window function, $J_o(x)$ is the Bessel function of the first kind of order zero, ζ_1 is the first zero of $J_o(x)$, and c is a measure of the degree to which high frequency components in the data are preserved in the smoothing process and is inversely related to the width of W_o. J_o can be accurately estimated (1 part in 10^7) by a polynomial approximation [12]. The parameter c controls the degree of smoothing produced by W_o. The effect of c on the window function can be seen in Fig. 5 where $W_o(\rho)$ is plotted for c values of 0.50, 0.30, and 0.10 as indicated in the figure. The effects of smoothing on the intensity data are shown in Fig. 6. The bottom curve of Fig. 6 shows the unsmoothed data while the top three curves correspond to increasing values of c. Complete removal of the structure due to grids is only accomplished using $c = 0.10$.

Influence of Extended Surface Structural on Oxidation of Al(111)

The surface structure has been characterized by LEED for six single crystal Al(111) surfaces following various preparation procedures. On each of these surfaces the molecular oxygen exposure and oxygen coverage for the onset of oxide nucleation has been determined by Auger electron spectroscopy. Simple chemisorption of oxygen on the surface was distinguished from oxide formation by monitoring both oxygen and aluminum Auger transitions. The oxygen Auger peak-to-peak height in a derivative spectrum ratioed to the corresponding aluminum peak (O/Al) was a measure of surface oxygen concentrations. Formation of aluminum oxide produces a change in shape of the aluminum Auger transition measured in the energy range 50 - 70 eV (see Fig. 7). In particular the main metallic peak at 68 eV transforms into a smaller peak at 54 eV. At low oxide concentrations the structure in the range 50 - 55 eV is a superposition of peaks due to the oxide and a metal plasmon loss peak at 52 eV. The onset of oxide formation is detected from the energy width of this satellite peak as measured by the peak-to-peak energy separation in the derivative spectrum. As shown in Fig. 8 this transition is very sharp as a function of oxygen exposure providing a clear indication of oxide formation. The exposures and O/Al ratios at the onset of oxidation for each of the surfaces studied are summarized in Table 1. The major structural defects on each surface are listed in column 2 and the exposures and oxygen O/Al Auger peak-to-peak height ratios are listed in columns 3 and 4, respectively. It is clear that surface steps accelerate the formation of oxide. All stepped surfaces (A, C, E and F) form oxide at lower oxygen exposures than surface B, the non-stepped surface. Fig. 9 shows a plot of the O/Al Auger ratio where oxide is first detected versus the surface step concentration. The oxygen

coverage required to nucleate oxide decreases monotonically as the step concentration increases from 0% to 12% and then remains approximately constant up to 25% steps. Table 2 lists approximate relative sticking probabilities for the six surfaces, normalized to surface B, the mosaic-covered, non-stepped surface. These sticking probabilities were calculated from the slope (linear least squares fits) of O/Al Auger peak-to-peak height ratios versus oxygen exposure obtained at low exposure. Direct measurements of sticking probabilities were not possible in these experiments. Within the uncertainty of the experimental measurements the sticking probabilities are independent of the step concentration.

Three possibilities for the influence of steps on oxide nucleation have been considered. 1) Steps may increase the sticking probability for molecular oxygen on the surface and thereby reduce the oxygen exposure required to reach the critical oxygen coverage required to nucleate oxide; 2) the critical oxygen coverage at steps may not be as high as on perfect terraces; and 3) steps may trap oxygen and thereby achieve the critical oxygen coverage locally before the oxygen coverage on the terraces reaches the critical value. An increase in sticking probability is clearly ruled on the basis of the data in Table 2. A lowering of the critical oxygen required to nucleate oxide is not in accord with the data in Fig. 9. A monotonic decrease in the average oxygen coverage at the onset of oxide formation with no leveling off is predicted by this model. The only possibility consistent with Fig. 9 is that oxide nucleation occurs at steps as a result of oxygen diffusion and clustering at step edges.

Diffuse LEED Measurements

During the last year we performed careful measurements of the background

intensity distribution between diffraction beams in a LEED pattern obtained from an Al(111) surface with submonolayer coverage of atomic oxygen. The measurements were performed using the digital, imaging LEED instrument developed in the first part of the research project. The purpose of these measurements is to evaluate the potential of whole-pattern LEED measurements for determining the detailed atomic structure of overlayers or point defects that have a single, uniform local atomic structure but which do not possess long range order across the surface. The O/Al(111) system is an ideal test system because 1) the overlayer atom has an atomic charge comparable to the substrate so that the scattering amplitude is also comparable; 2) there are no additional diffraction beams produced by oxygen adsorption and hence no long range order; 3) the local atomic structure is known from EXAFS and EELS measurements. Unfortunately, the whole pattern LEED measurements are dominated by a combination of structure in the microchannel plate detector and scattering in the retarding grids. The ridge structure observable in the diffraction pattern shown in Fig. 3 which appears to have the symmetry of the surface is in fact due to scattering of the strong diffraction beams by the grids of the electron optics. It may be possible to eliminate the detector artifacts by use of the Pendry Y-function. Efforts along these lines are still in progress.

REFERENCES

1. J.B. Pendry, Low Energy Electron Diffraction, Academic Press, London (1974).

2. M. Henzler, Surf. Sci. 73 (1978) 240.

3. D.G. Welkie, M.G. Lagally and R.L. Palmer, J. Vac. Sci. Technol. 17 (1980) 453.

4. M. Henzler, in Topics in Current Physics, Vol. 4, ed. H. Ibach, Springer-Verlag, Heidelberg (1977), 117.

5. R.L. Park, J. Appl. Phys. 37 (1966) 295.

6. J.B. Pendry and D.K. Saldin, Surf. Sci. 145 (1984) 33.

7. P.C. Stair, Rev. Sci. Instrum. 51 (1980) 132.

8. R.L. Park, J.E. Houston and D.G. Schreiner, Rev. Sci. Instrum. 42 (1971) 60.

9. T.M. Lu and M.G. Lagally, Surf. Sci. 99 (1980) 695.

10. K. Heinz, D.K. Saldin and J.B. Pendry, Phys. Rev. Lett. 55 (1985) 2312.

11. H. Stark and B. Dimitriadis, J. Opt. Soc. Am. 65 (1975) 425.

12. M. Abramowitz and I.A. Stegun, "Handbook of Mathematical Functions," NBS, 1964.

TABLE 1

Surface	Dominant Defect Structure	Initial Oxide Formation Exposure (L)	O/Al (±10%)
A	Step Arrays [step edge] = 3.3%	48	0.74
B	Mosaic Domains [mosaic edge] = 10%	47	0.93
C	Facets & Steps [step edge] = 12% [facets] = unknown	7	0.30
D	Dissolved Oxygen	9	0.40
E	Step Arrays [step edge] = 6%	40	0.46
F	Regular Steps Al(221) = 25% steps	14	0.34

TABLE 2

Surface	% Steps	Relative Sticking Probability
A	3.3	0.78
B	0	1.0
C	12	2.4
D	0	1.7
E	6	0.72
F	25	0.94

FIGURE CAPTIONS

Fig 1: Overview of the LEED/Auger ultrahigh vacuum instrument developed as part of the research.

Fig 2: Detailed schematic diagram of the digital, pulsed counting LEED optics.

Fig 3: Contour plot of the LEED pattern measured from a clean Al(111) surface.

Fig 4: A single line of intensity data from the two-dimensional digitized image of the LEED pattern of Al(111) before and after exposure to oxygen. Note the pattern of sharp structures which is common to the two intensity plots.

Fig 5: Plots of the optimum window function $W_o(\rho)$ for the indicated values of the width parameter c. The points indicate the discrete values of $W_o(\rho)$ actually used for smoothing.

Fig 6: Results of smoothing the clean Al(111) surface data shown in Fig. 4. Curve A is the unsmoothed data. Curves B - D correspond to values of the window width parameter of 0.1, 0.3, and 0.5 respectively.

Fig 7: Derivative Auger spectrum of the aluminum (MNN) transition from a clean metal surface, an oxide and a surface with a mixture of metal and oxide. The peak at 68 eV is assigned to metallic aluminum. The

small satellite peak at 52 eV in the clean surface spectrum is assigned to a plasmon loss. The peak at 54 eV is due to aluminum oxide.

Fig. 8: Peak-to-peak width of the satellite aluminum Auger feature as a function of oxygen exposure measured for surface C. Note the abrupt increase in width in the exposure range 7 to 10 L. The onset of oxide formation is taken to be at 7 L.

Fig. 9: Dependence of the O/Al Auger peak-to-peak height ratio on the concentration of surface steps.

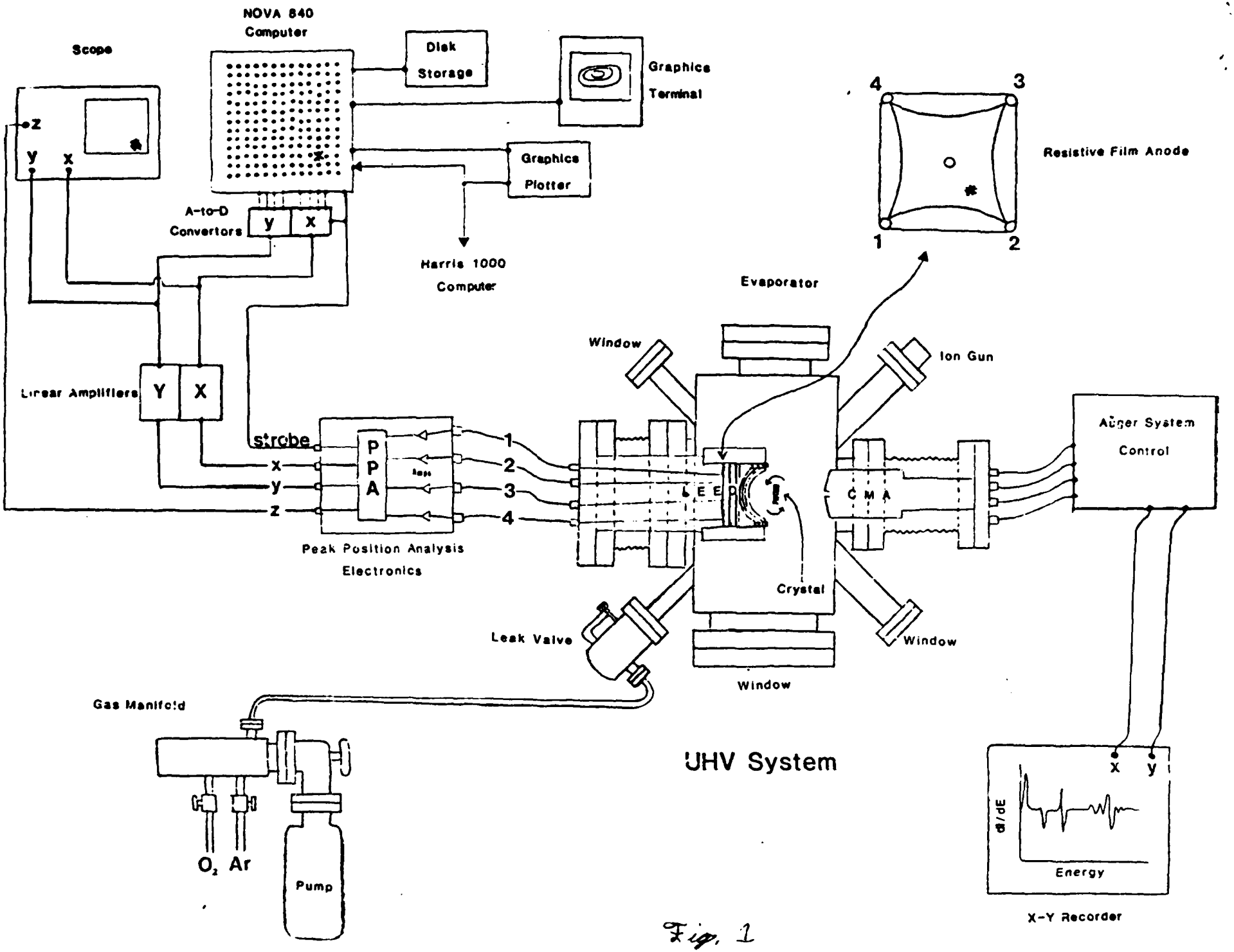
NOVA 840
Computer
Scope
Disk
Storage
Graphics
Terminal
Graphics
Plotter
Harris 1000
Computer
A-to-D
Convertors
Linear Amplifiers
Resistive Film Anode
Evaporator
Window
Ion Gun
strobe
Peak Position Analysis
Electronics
Auger System
Control
Crystal
Leak Valve
Window
Window
Gas Manifold
Pump
UHV System
Energy
X-Y Recorder

Fig. 1

Digital LEED Acquisition System

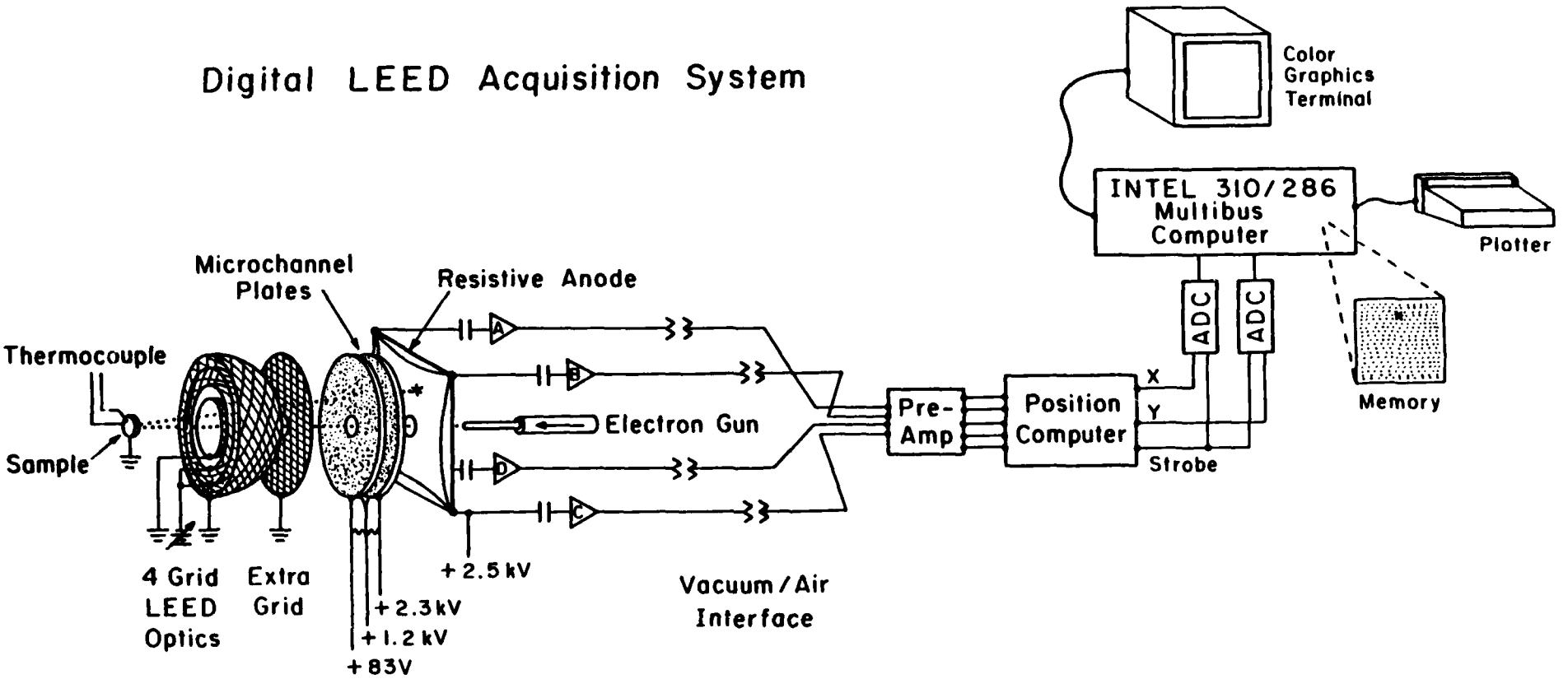

5000
6000
7000
8000
9000
10000
11000

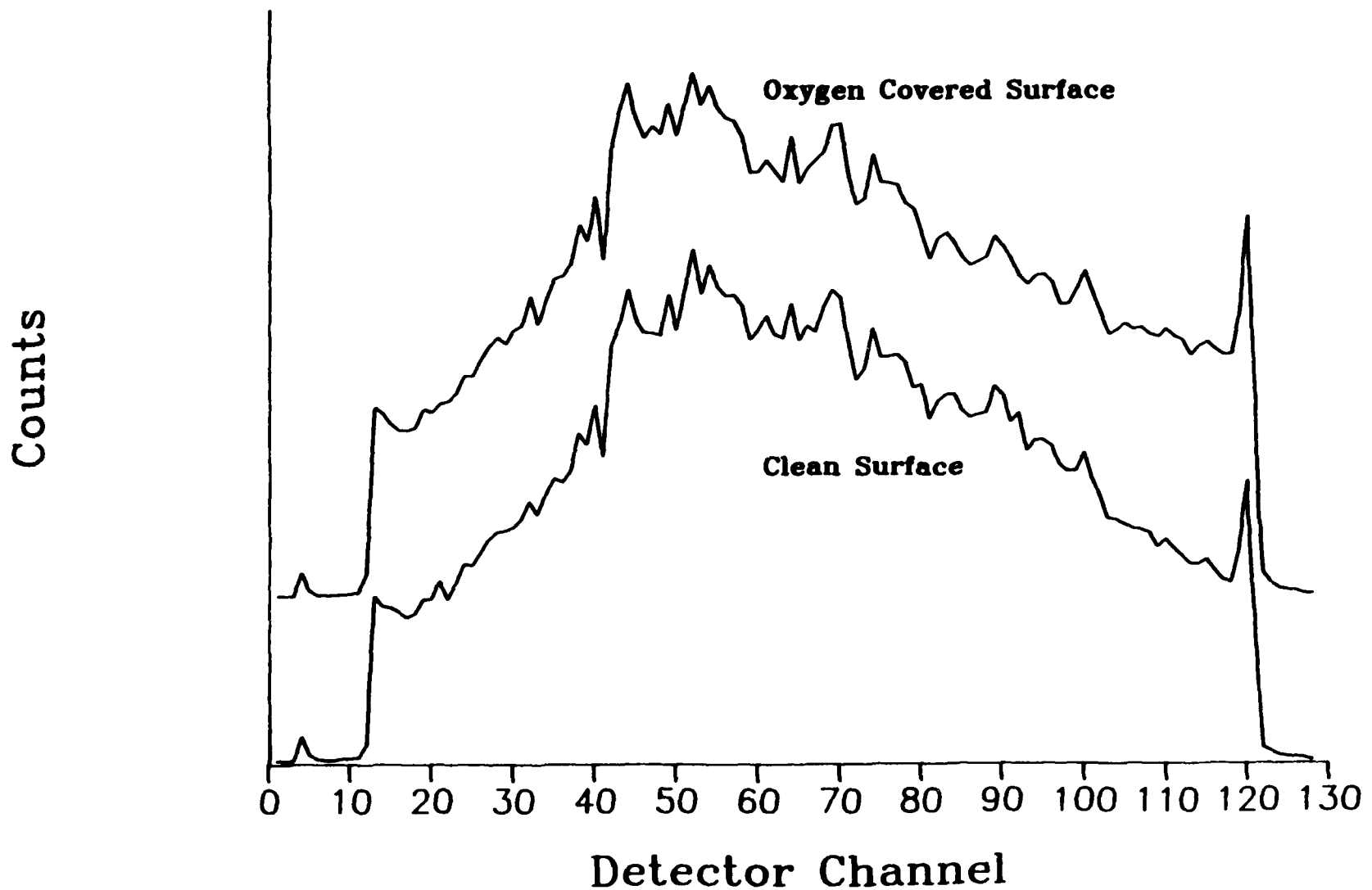
Oxygen Covered Surface
Clean Surface
Counts
0
10
20
30
40
50
60
70
80
90
100
110
120
130
Detector Channel

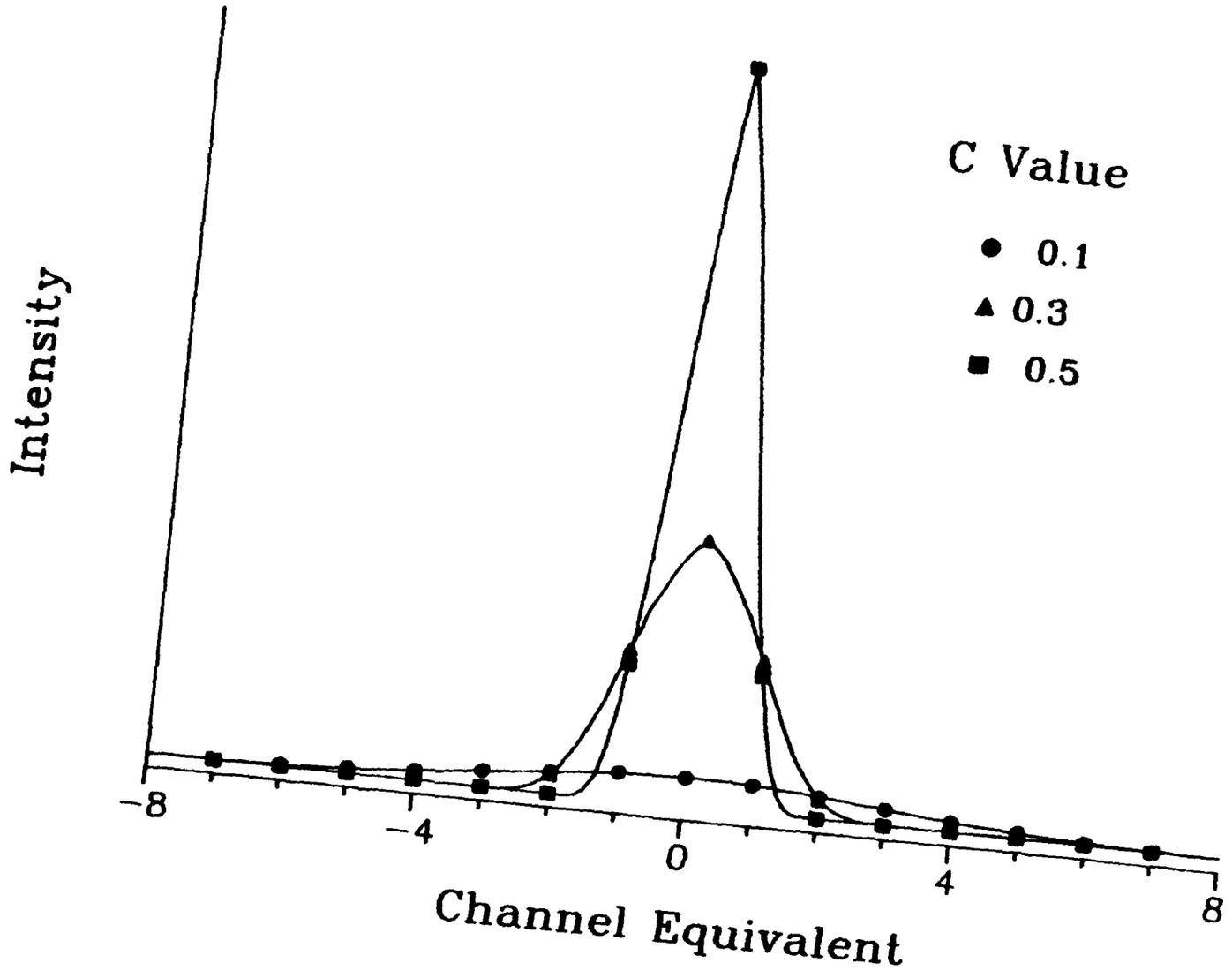
Intensity
C Value
0.1
0.3
0.5
−8
−4
0
4
8
Channel Equivalent

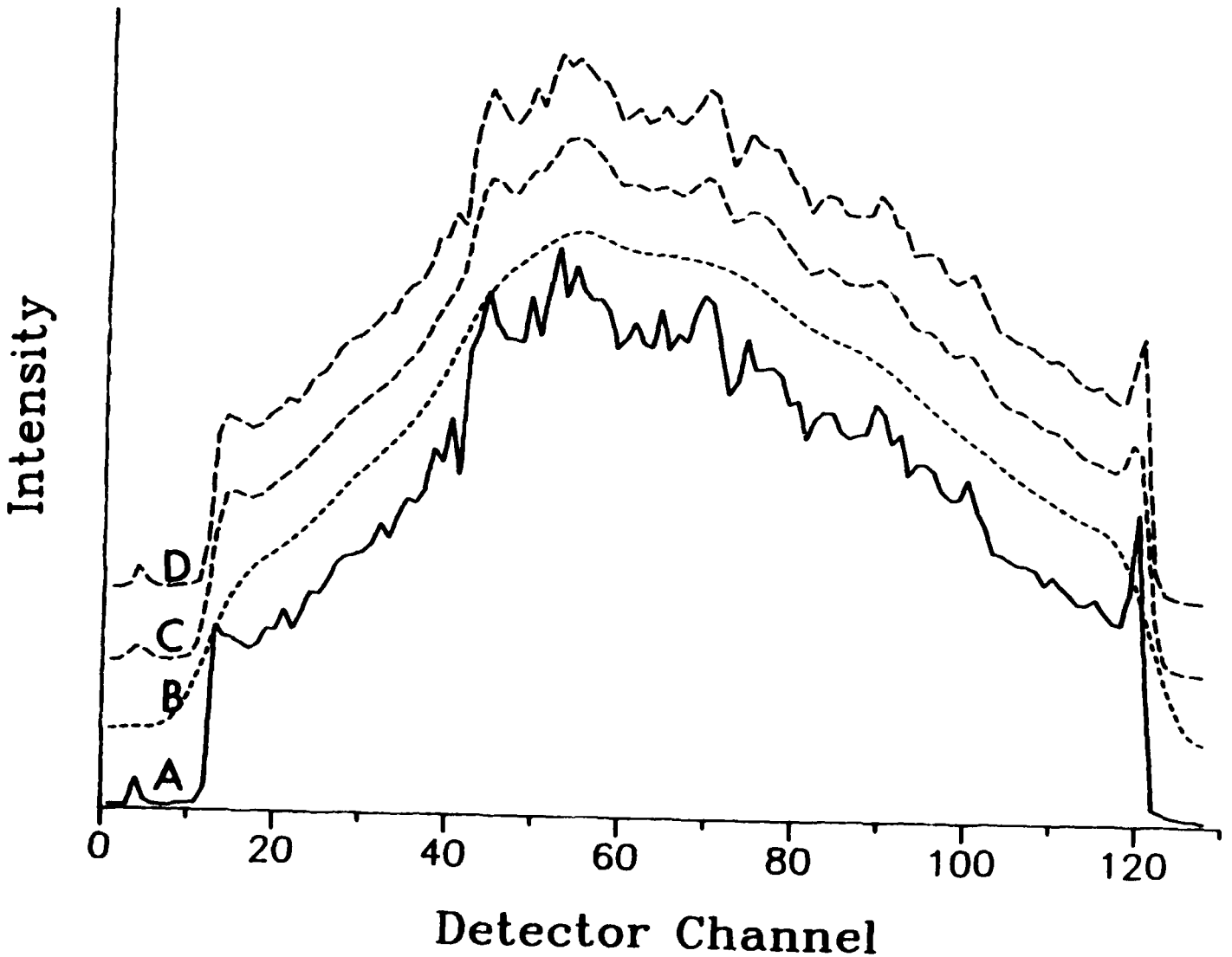
Intensity
D
C
B
A
0
20
40
60
80
100
120
Detector Channel

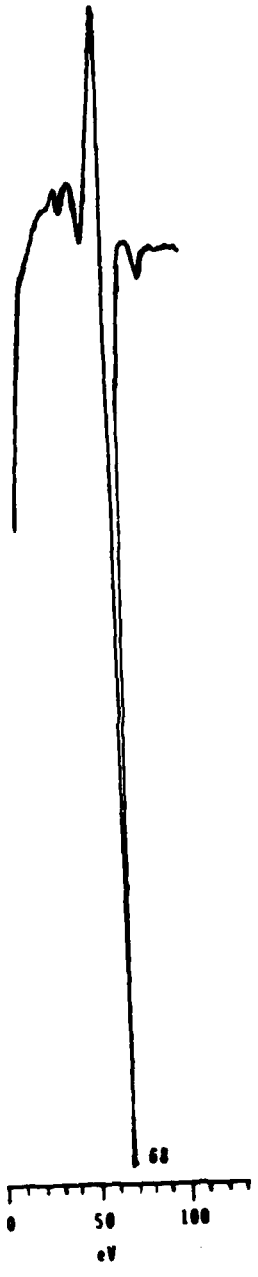

metal

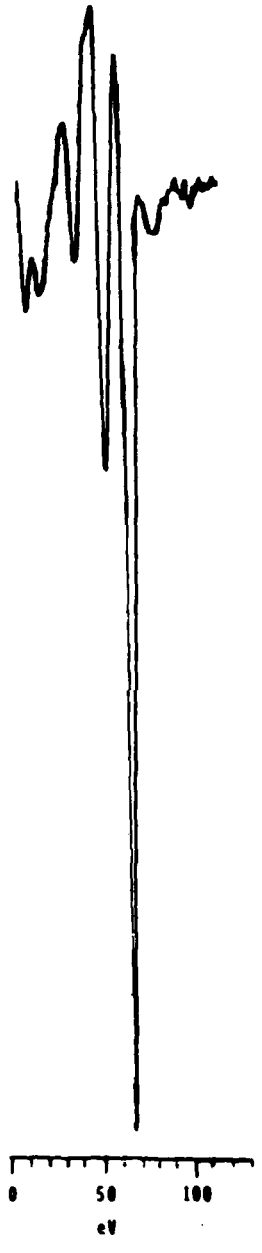

mixed

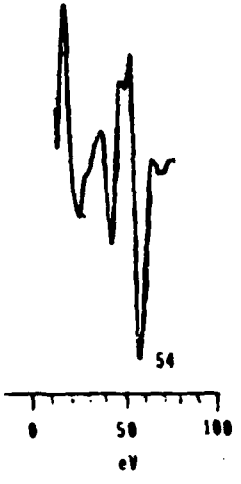

oxide

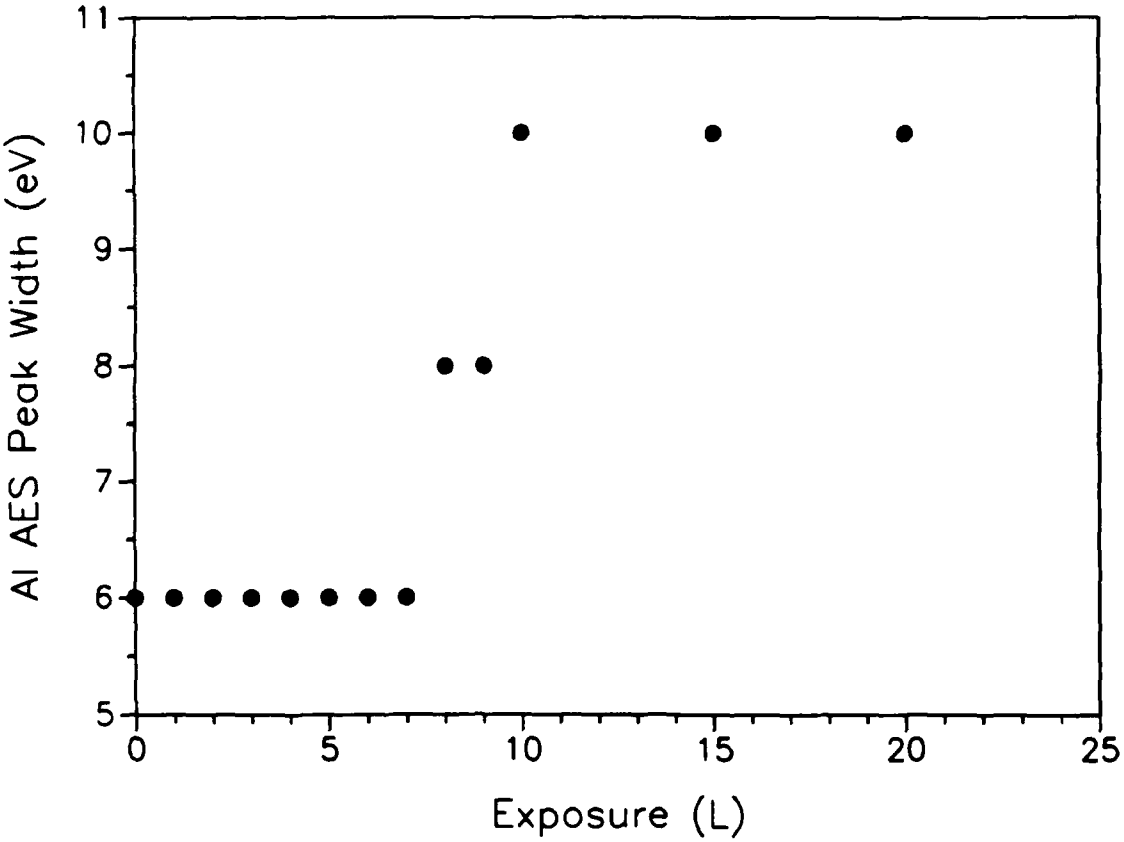
Al AES Peak Width (eV)
11
10
9
8
7
6
5
0
5
10
15
20
25
Exposure (L)

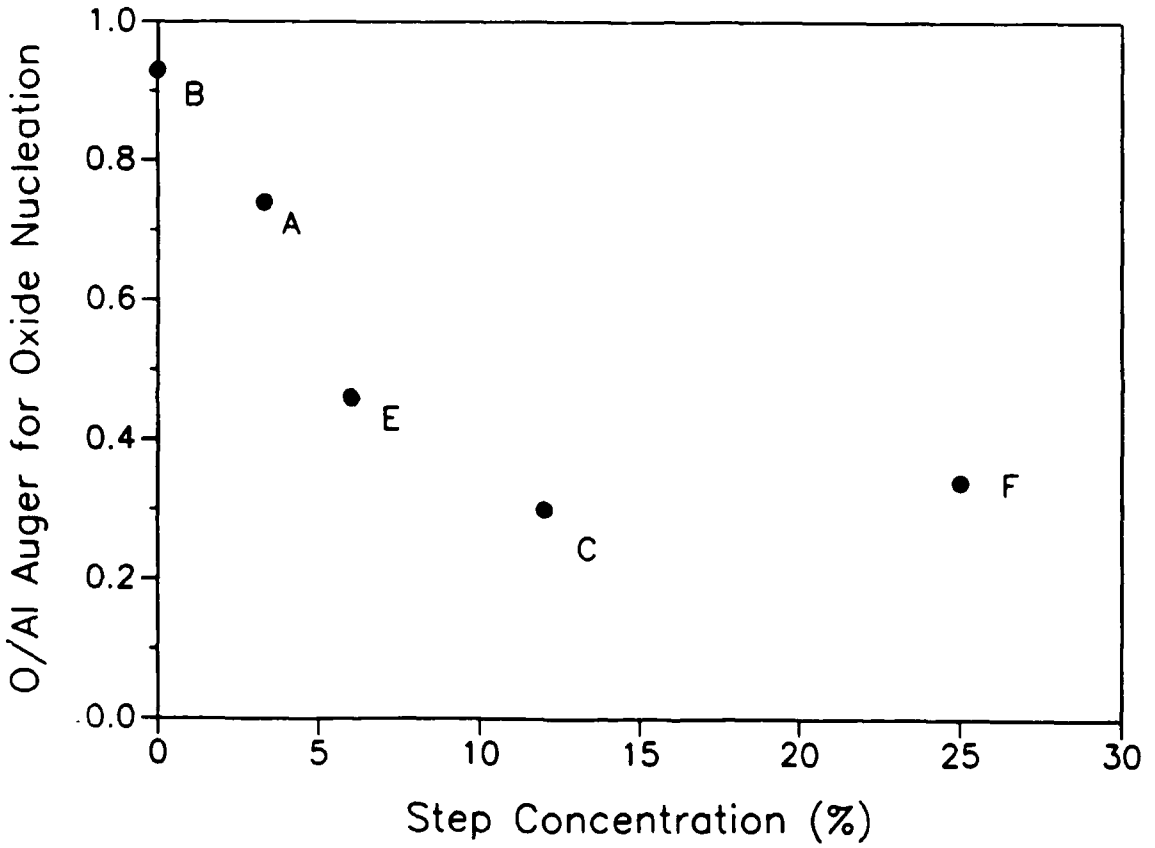
O/Al Auger for Oxide Nucleation
1.0
0.8
0.6
0.4
0.2
0.0
0
5
10
15
20
25
30
Step Concentration (%)
B
A
E
C
F

PUBLICATIONS

"The Effects of Surface Facets on the Oxidation of Aluminum (111) Surfaces," A.L. Testoni and P.C. Stair, Surface Science 171 (1986) L491.

"The Role of Surface Defects in Aluminum Surface Oxidation," A.L. Testoni and P.C. Stair, J. Vac. Sci. Technol. A4 (1986) 1430.

"Pulsed-Laser-Induced Desorption from Metal Surfaces,", Peter C. Stair and Eric Weitz, J. Opt. Soc. Am. B4 (1987) 255.

"The Role of Steps in the Oxidation of Al(111) Surfaces," A.L. Testoni and P.C. Stair, in preparation for Surface Science.

"The Instrument Response Function for a Digital Pulse Counting LEED Instrument," A.L. Testoni and P.C. Stair, in preparation for Rev. Sci. Instrum.

PERSONNEL

Principal Investigator: Professor Peter C. Stair

Graduate Research Assistants: Anne L. Testoni

John L. Grant

Jeffery Bruns

DEGREES AWARDED

Ph. D. - Chemistry

Anne Louise Testoni

June 1986

"Investigating the Role of Surface Structure on Surface Chemistry: The Oxidation of Single Crystal Aluminum Surfaces"

John Leonard Grant

June 1987

"Electronic Structure and Reactivity of Chemically Modified Mo(100) Surfaces and Application of Pulsed Laser Heating to Studies of Surface Chemical Phenomena"

PRESENTATIONS

"The Role of Surface Defects in Aluminum Surface Oxidation," 32nd National Symposium of the American Vacuum Society

"Dissociative Pathway Observed in Laser-Induced Thermal Desorption of CO from Cu(100)," 32nd National Symposium of the American Vacuum Society

"Digital LEED: Instrumentation and Applications," American Chemical Society National Meeting, Dallas, April 1989.